J Math Imaging Vis (2008) 30: 73–85
DOI 10.1007/s10851-007-0039-0

Measuring Elongation from Shape Boundary

Miloš Stojmenović · Joviša Žunić

Published online: 10 November 2007

Abstract Shape elongation is one of the basic shape descriptors that has a very clear intuitive meaning. That is the reason for its applicability in many shape classification tasks. In this paper we define a new method for computing shape elongation. The new measure is boundary based and uses all the boundary points. We start with shapes having polygonal boundaries. After that we extend the method to shapes with arbitrary boundaries. The new elongation measure converges when the assigned polygonal approximation converges toward a shape. We express the measure with closed formulas in both cases: for polygonal shapes and for arbitrary shapes. The new measure finds the elongation for shapes whose boundary is not extracted completely, which is impossible to achieve with area based measures.

Keywords Shape · Elongation · Orientation · Image processing · Computer vision · Early vision

1 Introduction

Shape descriptors are widely used in many image processing tasks. The demand for more efficient shape classification procedures is the reason for a permanent interest for newly created shape descriptors but also for new methods for measuring already created shape descriptors. The shape convexity is an example of shape descriptors with probably most different methods for its evaluation [2, 8, 11, 15, 21]. Most standard shape descriptors as they are compactness [17] and elongations are computable by closed formulas, but sometimes closed formulas are not possible and particular algorithms have to be created to evaluate defined shape descriptors [14]. If created algorithms do not have a low time complexity, then statistical methods for describing shapes could be involved [1, 11], as well.

In this paper we are focused on shape elongation problems. A new shape elongation measure will be introduced. Elongation has an intuitively clear meaning and is hence a very common shape descriptor. The standard measure of shape elongation is derived from the definition of shape orientation which is based on the axis of the last second moment of inertia. Precisely, the axis of the least second moment of inertia [6, 7, 9] is the line which minimizes the integral of the squares of distances of the points (belonging to the shape) to the line. The integral is defined as

$$I(S,\varphi,\rho)=\iint_S r^2(x,y,\varphi,\rho)dxdy \tag{1}$$

where $r(x,y,\varphi,\rho)$ is the perpendicular distance from the point (x,y) to the line given in the form

$$x\cdot\sin\varphi - y\cdot\cos\varphi=\rho.$$

The angle φ for which the integral $I(S,\varphi,\rho)$ reaches a minimum defines the orientation of the shape S. This angle is easy to compute. Elementary mathematics says that such an angle φ satisfies the following equation:

$$\frac{\sin(2\varphi)}{\cos(2\varphi)}=\frac{2\cdot\overline{m}_{1,1}(S)}{\overline{m}_{2,0}(S)-\overline{m}_{0,2}(S)}, \tag{2}$$

J. Žunić is also with the Mathematical Institute, Serbian Academy of Sciences and Arts, Belgrade.

M. Stojmenović
SITE, University of Ottawa, Ottawa, ON, K1N 6N5, Canada
e-mail: mstoj075@site.uottawa.ca

J. Žunić (✉)
Computer Science Department, Exeter University, Harrison Building, Exeter EX4 4QF, UK
e-mail: J.Zunic@ex.ac.uk

where $\overline{m}_{p,q}(S)$ are centralized moments of S defined as

$$\overline{m}_{p,q}(S) = \iint_S \left(x - \frac{\iint_S x dx dy}{\iint_S dx dy}\right)^p \cdot \left(y - \frac{\iint_S y dx dy}{\iint_S dx dy}\right)^q dx dy. \tag{3}$$

The minimum of $I(S, \varphi, \rho)$ is easy to compute:

$$\min_{\substack{\rho \geq 0 \\ \varphi \in [0,2\pi]}} \{I(S, \varphi, \rho)\} = \frac{\overline{m}_{2,0}(S) + \overline{m}_{0,2}(S) - \sqrt{4 \cdot (\overline{m}_{1,1}(S))^2 + (\overline{m}_{2,0}(S) - \overline{m}_{0,2}(S))^2}}{2}.$$

Notice that the minimum does not depend on ρ. This is in accordance with the fact that if $I(S, \varphi, \rho)$ reaches the minimum then $\rho = 0$—i.e. the axis of least second moment of inertia passes the origin.

If $\rho = 0$ is assumed then

$$\max_{\varphi \in [0,2\pi]} \{I(S, \varphi, \rho = 0)\} = \frac{\overline{m}_{2,0}(S) + \overline{m}_{0,2}(S) + \sqrt{4 \cdot (\overline{m}_{1,1}(S))^2 + (\overline{m}_{2,0}(S) - \overline{m}_{0,2}(S))^2}}{2}.$$

Next, the ratio between the extreme values $\max_{\varphi \in [0,\pi)} I(S, \varphi, \rho = 0)$ and $\min_{\varphi \in [0,\pi)} I(S, \varphi, \rho = 0)$

$$\mathcal{E}_{standard}(S) = \frac{\overline{m}_{2,0}(S) + \overline{m}_{0,2}(S) + \sqrt{4 \cdot (\overline{m}_{1,1}(S))^2 + (\overline{m}_{2,0}(S) - \overline{m}_{0,2}(S))^2}}{\overline{m}_{2,0}(S) + \overline{m}_{0,2}(S) - \sqrt{4 \cdot (\overline{m}_{1,1}(S))^2 + (\overline{m}_{2,0}(S) - \overline{m}_{0,2}(S))^2}}. \tag{4}$$

is the standard measure (i.e. most quoted in literature) of elongation of the shape S. Some generalization of the standard method for measuring shape elongation can be found in [19]. Let us mention that there are also some naive measures of elongation. For example, shape elongation can be measured as the ratio of the longer and shorter edges of the minimum area bounding rectangle for the measured shape. It is worth mentioning that such bounding rectangles are easy to compute [5, 10].

The standard measure (4) of shape elongation is area based because all points belonging to the shape are involved in the computation (area moments are used). Our new shape elongation measure is boundary based. Only the boundary points are used for computation and consequently, the measure strongly depends on boundary defects, caused by noise or narrow shapes intrusions, for example. On the other hand, as a sensitive measure, the new measure could be more suitable for high precision tasks, for high quality images, or if working whit shapes whose inherent characteristics are deep intrusions and their positions inside shape.

In this paper we will use this standard approach "from-orientation-to-elongation" along with a recently disclosed method for computing shape orientation [20, 22] to derive the new measure for shape elongation.

The paper is organized as follows. A short overview of the recently derived method for shape orientation computation [20, 22] is given in Sect. 2. Section 3 gives the new elongation measure for shapes with polygonal boundaries. In Sect. 4 we extend the method to shapes with arbitrary boundaries. Experimental results and illustrations are given in Sect. 5, while Sect. 6 gives concluding remarks.

2 Boundary Based Shape Orientation

As mentioned, we will derive a new shape elongation measure from a recent [22] boundary based method for computing the orientation of polygonal shapes. We will first give a short sketch of the main result from [22]. Let P be a polygon and let $|\mathbf{pr}_{\vec{a}}(e)|$ denote the length of the projection of the edge e of P onto a line parallel to the vector $\vec{a} = (\cos\alpha, \sin\alpha)$. Then, roughly speaking, the authors of [22] consider a variety of functions

$$F_{p,q}(\alpha, P) = \sum_{e \text{ is an edge of } P} \frac{|\mathbf{pr}_{\vec{a}}(e)|^p}{|e|^q}$$

and define the orientation of P by the angle for which $F_{p,q}(\alpha, P)$ reaches the maximum.

The choice of exponents p and q depends on the required purpose of the formula. If $p = 2$ and $q = 0$, i.e., $F_{2,0}(\alpha, P) = \sum_{e \text{ is an edge of } P} |\mathbf{pr}_{\vec{a}}(e)|^2$, the orientation is defined by the angle α that maximizes the sum of the squared lengths of the projections of all the edges of P onto a line having slope α.

However, $F_{2,0}(\alpha, P)$ does not satisfy the "convergence" property. A recent article ([16]) proposed an elongation measure for polygons based on $F_{2,0}(\alpha, P)$. Since the underlying orientation calculation did not converge, the elon-

gation measure did not converge either. This article develops an alternative elongation measure based on $F_{2,1}(\alpha, P)$ and proves its convergence. More precisely, let a polygonal curve be represented in parametric form as $x = x(t)$, $y = y(t)$, for $t \in [a, b]$. Let a sequence $t_1 = a < t_2 < \cdots < t_{k-1} < t_k = b$ and let $P(t_1, \ldots, t_k)$ be a polygonal line (not necessarily open) whose vertices are $(x(t_1), y(t_1)) = (x(a), y(a))$, $(x(t_2), y(t_2)), \ldots, (x(t_{k-1}), y(t_{k-1}))$, $(x(t_k), y(t_k)) = (x(b), y(b))$. Then the "convergence" property would mean that for an increasing k and an arbitrary choice of the sequence $t_1 = a < t_2 < \cdots < t_{k-1} < t_k = b$ such that the maximum distance between the consecutive points $(x(t_i), y(t_i))$ and $(x(t_{i+1}), y(t_{i+1}))$, $(1 \le i < k-1)$ tends to zero, the computed orientations of the polygonal lines $P(t_1, \ldots, t_k)$ converge to the same value. A big disadvantage (particularly when working with shapes with 'smooth curved' boundaries) is that the shape orientation defined by the maxima of $F_{2,0}(\alpha, S)$ does not have such a convergence property. On the other hand, convergence is guaranteed for $F_{2,1}(\alpha, P)$ (as proven in [22]).

The paper [22] gives a preference to the method based on the use of $F_{2,1}(\alpha, P)$ when the orientation is computed. There are two strong reasons for this:

- a closed formula for the computation of the orientation of P is enabled;
- such a computed orientation satisfies the convergence property.

So, in the rest of this paper, we will derive a new elongation measure considering the function $F_{2,1}(\alpha, P)$.

Next, we will show how shape orientation can be computed based on $F_{2,1}(\alpha, P)$. We start with a formal definition.

Definition 2.1 Let P be a planar shape with a polygonal boundary, and let $\overrightarrow{a} = (\cos\alpha, \sin\alpha)$ denote the unit vector with direction α. Then, the orientation of the shape is defined by the angle α such that the total sum

$$F_{2,1}(\alpha, P) = \sum_{e \text{ is an edge of } P} \frac{|\mathbf{pr}_{\overrightarrow{a}}(e)|^2}{|e|} \tag{5}$$

is maximal possible.

Notice that the summands in (5) are squared lengths of projections of the edges of P (onto a line having slope α) divided by the edge lengths.

Because the length of the projection $\mathbf{pr}_{\overrightarrow{a}}(e_i)$ of the edge e_i onto a line having slope α is

$$\begin{aligned} |\mathbf{pr}_{\overrightarrow{a}}(e_i)| &= |e_i| \cdot |(\cos\alpha_i \cos\alpha + \sin\alpha_i \sin\alpha)| \\ &= |e_i||\cos(\alpha_i - \alpha)|, \end{aligned}$$

the function $F_{2,1}(\alpha, P)$ can be expressed as

$$F_{2,1}(\alpha, P) = \sum_{i=1}^{n} \frac{|\mathbf{pr}_{\overrightarrow{a}}(e_i)|^2}{|e_i|} = \sum_{i=1}^{n} |e_i| \cos^2(\alpha_i - a). \tag{6}$$

By setting the first derivative $dF_{2,1}(\alpha, P)/d\alpha$ equal to zero

$$\begin{aligned} &\frac{dF_{2,1}(\alpha, P)}{d\alpha} \\ &= \sum_{i=1}^{n} |e_i| \cdot \sin(2\alpha_i - 2\alpha) \\ &= \sum_{i=1}^{n} |e_i| \cdot (\sin(2\alpha_i)\cos(2\alpha) - \cos(2\alpha_i)\sin(2\alpha)) \\ &= 0 \end{aligned} \tag{7}$$

we derive that both angles for which $F_{2,1}(\alpha, P)$ reaches its minimum and maximum satisfy

$$\frac{\sin(2\alpha)}{\cos(2\alpha)} = \frac{\sum_{i=1}^{n} |e_i| \sin(2\alpha_i)}{\sum_{i=1}^{n} |e_i| \cos(2\alpha_i)}. \tag{8}$$

Thus, the orientation of a given polygonal shape P is very easy to compute in accordance with the equality (8). In the next section we compute both maxima and minima of $F_{2,1}(\alpha, P)$ and use their ratio as a new elongation measure.

Remark 2.1 In the case of a very fine polygonal approximation of a real curve the edges from this approximation are expected to be very short. But as small edge lengths are assumed, i.e. even if $\max|e| \to 0$ we do not have the 'dividing by zero' problem in (5). That is obvious from (6), which is actually equivalent to (5). Under the same assumption (i.e. $\max|e| \to 0$) both $\max F_{2,1}(\alpha, P)$ and $\min F_{2,1}(\alpha, P)$ tend to zero. But for a fixed P angles for which $F(\alpha, P)$ reaches the minimum and maximum are still well defined, independently of $\max|e|$. In the rest of paper we will consider the ratio between $\max F_{2,1}(\alpha, P)$ and $\min F_{2,1}(\alpha, P)$, and will show that this ratio converges, providing that all the vertices of P belong to a piecevise smooth curve and $\max|e| \to 0$.

3 New Shape Elongation Measure for Polygonal Shapes

In this section we consider the elongation of shapes having polygonal boundaries. Let us mention that, generally speaking, the restriction to polygonal shapes is not strictly enforced since real image processing applications deal with discrete data that are a result of a particular discretization process. In order to enhance the data manipulation, the boundaries of the original shapes are usually approximated with canonical arc sections (circular arcs, parabolic arcs, straight line segments, etc.). Approximating boundaries by straight line sections (i.e., polygonal approxima-

tion) is used most frequently and many algorithms for the polygonal shape approximation already exist—see [13].

Following the idea of the standard method for measuring shape elongation we define the new elongation measure as the ratio of the maximum and minimum value of the function that has been used for computing the shape orientation. We give the following definition.

Definition 3.1 Let P be a shape with a polygonal boundary. Then, the elongation of P is defined as the ratio

$$\mathcal{E}(P) = \frac{\max\{F_{2,1}(\alpha, P) \mid \varphi \in [0, 2\pi]\}}{\min\{F_{2,1}(\alpha, P) \mid \varphi \in [0, 2\pi]\}} \tag{9}$$

of the maximum and minimum of the function $F_{2,1}(\alpha, P)$.

For practical applications it would be a desirable property if $\mathcal{E}(P)$ is easily computable. The next theorem shows that the computation is simple, and more over it turns out that there is a closed formula for the computing shape elongation as defined by (8) from Definition 3.1.

Theorem 3.1 *Let P be a shape with a polygonal boundary. Then the new elongation measure of P can be expressed as*

$$\mathcal{E}(P) = \frac{\sum_{1\le i\le n} |e_i| + \sqrt{(\sum_{1\le i\le n} |e_i|\cos(2\alpha_i))^2 + (\sum_{1\le i\le n} |e_i|\cdot\sin(2\alpha_i))^2}}{\sum_{1\le i\le n} |e_i| - \sqrt{(\sum_{1\le i\le n} |e_i|\cdot\cos(2\alpha_i))^2 + (\sum_{1\le i\le n} |e_i|\cdot\sin(2\alpha_i))^2}} \tag{10}$$

where e_i $(1 \le i \le n)$ are edges of the boundary of P and α_i $(1 \le i \le n)$ are angles between the edges e_i and the x-axis.

Proof By using a simple trigonometric identity $\cos^2(\alpha) = \frac{1+\cos 2\alpha}{2}$ we can transform the optimizing function $F_{2,1}(\alpha, P)$ from the form (6) into:

$$F_{2,1}(\alpha, P) = \frac{1}{2}\cdot\sum_{1\le i\le n} |e_i| + \frac{1}{2}\cdot\sum_{1\le i\le n} |e_i|(\cos(2\alpha_i)\cos(2\alpha) + \sin(2\alpha_i)\sin(2\alpha)). \tag{11}$$

As already proved (see (8)), the angle values γ for which $F_{2,1}(\alpha, P)$ reaches its minimum and maximum satisfy

$$\frac{\sin(2\gamma)}{\cos(2\gamma)} = \frac{\sum_{i=1}^{n} |e_i|\sin(2\alpha_i)}{\sum_{i=1}^{n} |e_i|\cos(2\alpha_i)}.$$

Now, using the trigonometric identities:

$$\sin(2\varphi) = \frac{\pm\tan(2\varphi)}{\sqrt{1+\tan^2(2\varphi)}} \quad \text{and} \quad \cos(2\varphi) = \frac{\pm 1}{\sqrt{1+\tan^2(2\varphi)}}$$

we derive that $\cos(2\gamma)$ and $\sin(2\gamma)$ at the extreme points of $F_{2,1}(\alpha, P)$ can be expressed (together) as

$$\cos(2\gamma) = \frac{\pm\sum_{1\le i\le n} |e_i|\cos(2\alpha_i)}{\sqrt{(\sum_{1\le i\le n} |e_i|\cos(2\alpha_i))^2 + (\sum_{1\le i\le n} |e_i|\sin(2\alpha_i))^2}}$$

and

$$\sin(2\gamma) = \frac{\pm\sum_{1\le i\le n} |e_i|\sin(2\alpha_i)}{\sqrt{(\sum_{1\le i\le n} |e_i|\cos(2\alpha_i))^2 + (\sum_{1\le i\le n} |e_i|\sin(2\alpha_i))^2}}.$$

Entering the last two equalities into (11) we derive that the minimum and maximum of $F_{2,1}(\alpha, P)$ can be expressed as

$$\frac{1}{2}\sum_{1\le i\le n}|e_i| + \frac{1}{2}\cdot\sum_{1\le i\le n}|e_i|\cdot\frac{\pm\cos(2\alpha_i)\cdot\sum_{1\le i\le n}|e_i|\cos(2\alpha_i)}{\sqrt{(\sum_{1\le i\le n}|e_i|\cos(2\alpha_i))^2+(\sum_{1\le i\le n}|e_i|\sin(2\alpha_i))^2}}$$
$$+\frac{1}{2}\cdot\sum_{1\le i\le n}|e_i|\cdot\frac{\pm\sin(2\alpha_i)\cdot\sum_{1\le i\le n}|e_i|\sin(2\alpha_i)}{\sqrt{(\sum_{1\le i\le n}|e_i|\cos(2\alpha_i))^2+(\sum_{1\le i\le n}|e_i|\sin(2\alpha_i))^2}}$$

or equivalently as

$$\frac{1}{2}\cdot\sum_{1\le i\le n}|e_i| \pm \frac{1}{2}\cdot\frac{(\sum_{1\le i\le n}|e_i|\cos(2\alpha_i))^2+(\sum_{1\le i\le n}|e_i|\sin(2\alpha_i))^2}{\sqrt{(\sum_{1\le i\le n}|e_i|\cos(2\alpha_i))^2+(\sum_{1\le i\le n}|e_i|\sin(2\alpha_i))^2}}.$$

Thus, we derived that the maximum and minimum of $F_{2,1}(\alpha, P)$ are as follows:

$$\max\{F_{2,1}(\alpha,P)\mid\varphi\in[0,2\pi]\} = \frac{1}{2}\cdot\sum_{1\le i\le n}|e_i| + \frac{1}{2}\cdot\sqrt{\left(\sum_{1\le i\le n}|e_i|\cdot\cos(2\alpha_i)\right)^2+\left(\sum_{1\le i\le n}|e_i|\cdot\sin(2\alpha_i)\right)^2}$$
$$\min\{F_{2,1}(\alpha,P)\mid\varphi\in[0,2\pi]\} = \frac{1}{2}\cdot\sum_{1\le i\le n}|e_i| - \frac{1}{2}\cdot\sqrt{\left(\sum_{1\le i\le n}|e_i|\cdot\cos(2\alpha_i)\right)^2+\left(\sum_{1\le i\le n}|e_i|\cdot\sin(2\alpha_i)\right)^2}. \quad (12)$$

This establishes the proof. □

Theorem 3.1 (i.e. the equality (10)) shows that the new elongation measure is easy to compute. Lemma 3.1 lists two more properties that encompass the new elongation measure. The proof is omitted because it follows directly from the definitions.

Lemma 3.1 *The new elongation measure satisfies the following properties*:

(i) $\mathcal{E}(P)\in[1,\infty)$ *for each polygonal shape* P;
(ii) $\mathcal{E}(P)$ *is invariant with respect to similarity transformations*.

Notice that $\mathcal{E}(P)$ is not given in a normalized form, i.e., as a quantity from the interval $[0,1]$ (see the item (i) of Lemma 3.1). We will not use a normalization procedure in order to be able to compare our results to the standard elongation measure that is also not normalized and has the range from 1 to infinity.

Remark 3.1 It is worth mentioning that the new elongation measure is valid for both open and closed polygonal lines. Also, it can be applied to a set of several polygonal lines. This enables the method to be applicable to shapes whose boundaries are not completely extracted—see Fig. 3. The reasons for an incompletely extracted boundary could be: the shape is partially overlaid, there are large similarities between background pixels and pixels belonging to the shape, etc.

4 Experimental Results

In the previous section we proposed a new shape elongation measure for polygonal shapes. The measure is naturally motivated and simple to compute. There is a closed formula (10) that expresses the elongation of a given polygonal shape as a function of the boundary edges and angles that those edges make with the x-axis. It performs well in some standard cases. For example, let us consider a rectangle $R(a)$ having edge lengths a and 1. In accordance with (10) its measured elongation is

$$\mathcal{E}(R(a)) = \frac{1+a+\sqrt{(a-1)^2}}{1+a-\sqrt{(a-1)^2}} = \begin{cases} a & \text{if } a>1,\\ 1 & \text{if } a=1,\\ 1/a & \text{if } a<1\end{cases}$$

which is acceptable. In the limit cases where either $a\to\infty$ or $a\to 0$ the rectangle degenerates into a line segment while the measured elongations tend to infinity. This behavior is expected, and in fact preferred. In the case of $a=1$ the measured elongation is equal to 1. In this case the rectangle degenerates into a square which is a 4-fold rotationally symmetric shape. Problems arising when working with manifold rotationally symmetric shapes are discussed in [18, 19].

Next, we give several shapes with their measured elongations.

In Fig. 1 boundaries of 10 fish images are approximated by polygonal lines. The boundaries appear in increasing sorted order with respect to their measured elongations. The

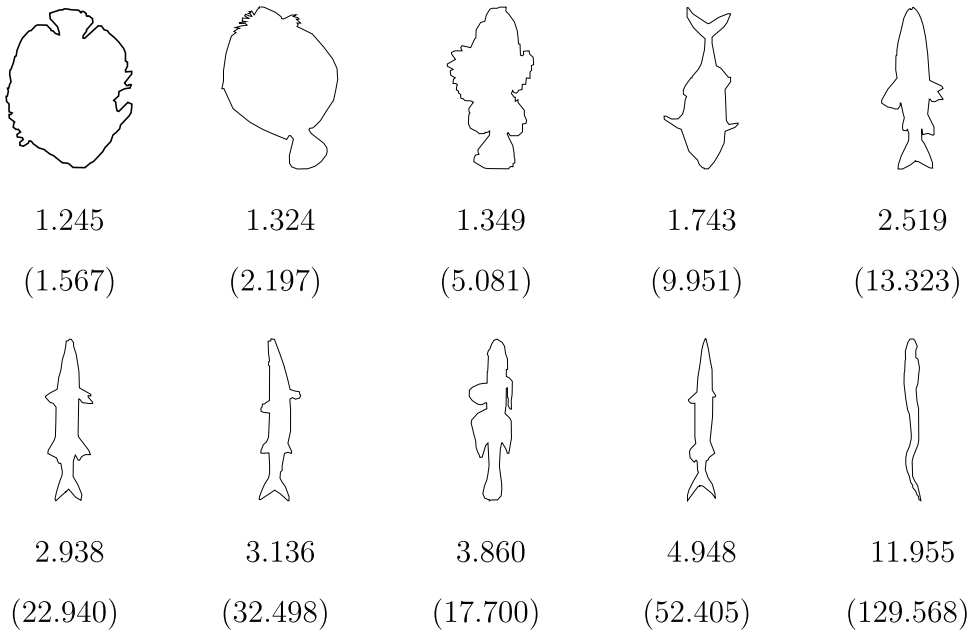

Fig. 1 Computed elongations by the new method. Elongations computed by the standard method are in brackets

measured standard elongations are given in the brackets. The ranking is as expected and both measures give almost the same ranking. There is only one exception. The third shape in the second row is ranked 8th with respect to the new measure, while it is ranked 6th by the standard elongation measure. If this shape is omitted the rest of shapes have the same ranking with respect to both measures. Such a higher measured elongation (by the new measure) in the case of the third shape in the second row is caused mainly by sharp the intrusions on right side of the shape boundary.

Several shapes presented in Fig. 2 are given in order to illustrate the nature of the new measure. The first two shapes, (a) and (b), have almost the same measured elongation if the standard measure is used. If a new measure is used there is an essential difference in the measured elongations. That is caused by the fact that the new measure is boundary based and deep intrusions into a shape have a big impact on the measured elongation. Shapes (c) and (d) illustrate how shape change could lead to different ranking if $\mathcal{E}$ and $\mathcal{E}_{standard}$ are applied. This change in the ranking order of shapes (c) and (d) (measured by the new elongations measure) is probably not preferred as the change in the ranking order for the shapes (a) and (b). A lower new elongation measure of the shape (c) could be explained by the fact that the function $F_{2,1}(\alpha, P)$, in this a particular case, reaches the minimum for $\alpha = 100°$. For such an angle, the most edges of the shape (c) are either nearly orthogonal or nearly vertical to a line having such a direction and the ration of max $F_{2,1}(\alpha, P)$ and min $F_{2,1}(\alpha, P)$ is more distinct than in the case of shape (d). Shapes (e) and (f) illustrate that an intrusion has a bigger impact on the measured elongation if it is along the direction of the shape orientation.

Shapes (g)–(i) illustrate an interesting property of the new measure. Namely, if a compound shape consists of several shapes with the same elongation and if those shapes have the same orientation, then the adding another shape with the same elongation and the same orientation does not change the elongation of such a compound shape. Indeed, shapes (g) and (i) have the same measured elongation. Shape (h) has almost the same elongation. The small man silhouette is not just a result of the scaling of a big man silhouette, which causes a slight difference in the measure. Since the standard elongation measure does not have such a property, the measured elongations (g)–(i) are essentially different. A similar explanation is valid for shapes (j)–(k). Since all three air-planes from the figure (k) can be obtained as a scaling transformation of the shape (j) and because they have the same orientation, then the measured elongations coincide. The obtained elongation in the figure (l) is differs from (j) and (k) because the air-planes in figure (l) do not have the same orientation. Such a new measured elongation can be useful in certain applications (when dealing with clusters of similar objects—e.g. flock of birds, shoal of fish, etc.) particularly if combined with the corresponding elongation measured on the standard way.

We formulate this interesting property as a lemma.

Lemma 4.1 *Let a compound shape S consist of several shapes $S_1, \ldots, S_m$. If all shapes $S_1, \ldots, S_m$ have the same orientation and the same elongation, both computed by a use of $F_{2,1}(S)$ then the computed elongation of S is consistent with elongations of the shapes $S_1, \ldots, S_m$, i.e., $\mathcal{E}(S) = \mathcal{E}(S_1) = \cdots = \mathcal{E}(S_m)$.*

Proof The proof follows directly from the definition. □

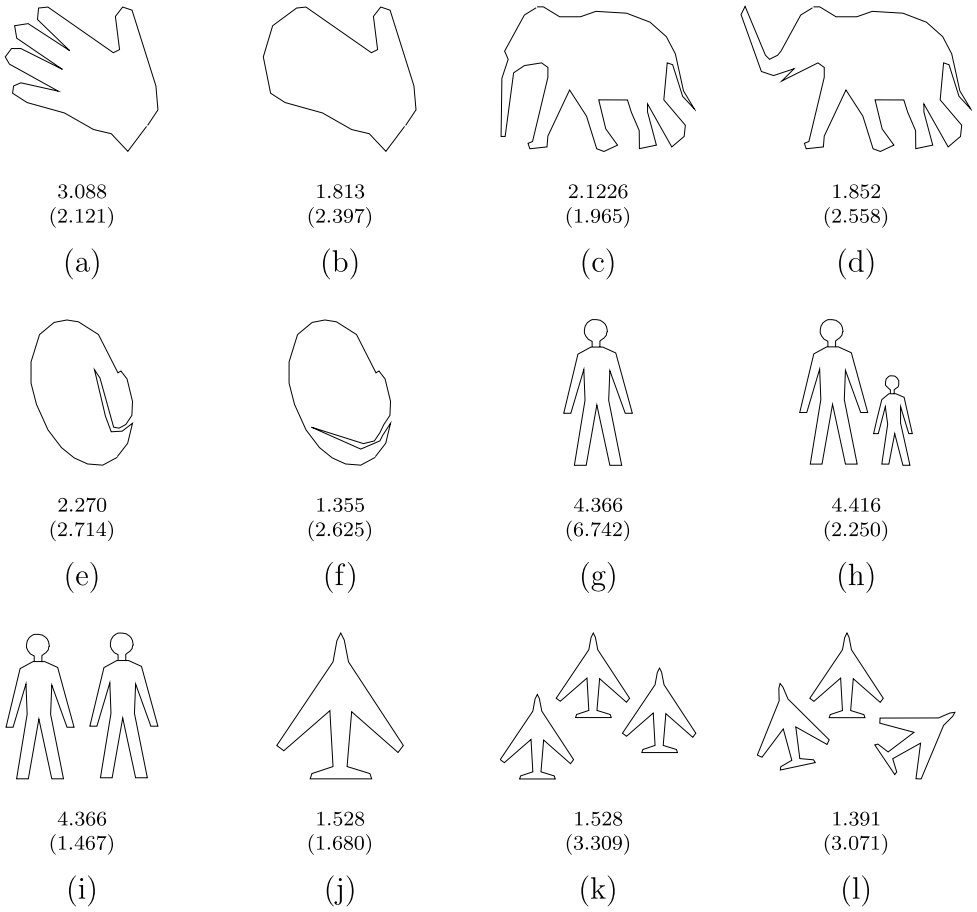

Fig. 2 Computed elongations by the new method. Elongations computed by the standard method are in brackets

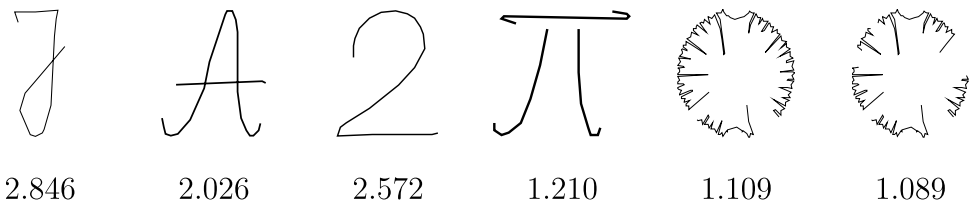

Fig. 3 Computed elongations of objects composed by one or several curve segment parts. The new method is applied

We conclude this section with shapes that are presented by partially detected boundaries and with shapes that are assumed to be presented by curve segments. Such examples are given in Fig. 3. The standard method cannot be applied in the presented situations.

5 Elongation of Shapes with Arbitrary Boundaries

In this section we extend the new elongation measure to shapes with arbitrary boundaries. First, we will show that the measure $\mathcal{E}(P)$ satisfies the "convergence property". Precisely, let us assume we have a curve and a set of sample points from it. Also, let us assume that we have the computed elongation of the polygonal curve whose vertices are the selected sample points. Then, roughly speaking, by the convergence property of an elongation measure we mean that the computed elongations (of polygonal curves determined by sample points) should converge when the density of sample points increases. Naturally, if the convergence property holds, the limit value for the measured elongations of polygonal lines determined by sample points is used as the elongation measure of the sampled curve.

To prove the convergence property of $\mathcal{E}(P)$ we need the following simple identities

$$\sin(2\alpha) = \frac{2\tan\alpha}{1+\tan^2\alpha}, \qquad \cos(2\alpha) = \frac{1-\tan^2\alpha}{1+\tan^2\alpha} \tag{13}$$

and the following statement from integral calculus.

Statement 1 *Let ρ be a piecewise smooth enough curve given in parametric form $x = x(t)$, $y = y(t)$ where $t \in [a, b]$. Let*

$$A_1 = (x(t=a), y(t=a)), \quad A_2, \quad \ldots, \quad A_{k-1},$$
$$A_k = (x(t=b), y(t=b))$$

be points from the curve ρ while a point $\tilde{A}_i$ is from the arc segment A_iA_{i+1}. Also, let $f(x, y)$ be a continuous, piecewise sufficiently differentiable, function. Then $\sum_{i=1}^{k-1} f(x, y) \cdot |A_iA_{i+1}|$ converges if $\max\{|A_iA_{i+1}|, 1 \le i < k\} \to 0$ is provided. More formally

$$\lim_{\max\{|A_iA_{i+1}|, 1\le i<k\}\to 0} \sum_{i=1}^{k-1} f(\tilde{A}_i) \cdot |A_iA_{i+1}|$$
$$= \oint_\rho f(x, y)ds = \int_a^b f(x(t), y(t))\sqrt{\dot{x}^2 + \dot{y}^2}dt. \qquad (14)$$

Now, we give the main result of this paper that gives a formula for computation of the new shape elongation measure for shapes having arbitrary boundaries. A particular case of this new formula is the formula (10) which holds for shapes with polygonal boundaries.

Theorem 5.1 *Let ρ be a piecewise smooth enough curve given in parametric form $x = x(t)$, $y = y(t)$ where $t \in [a, b]$. Let*

$$A_1 = (x(t=a), y(t=a)), \quad A_2, \quad \ldots, \quad A_{k-1},$$
$$A_k = (x(t=b), y(t=b))$$

be points from the curve ρ and let $P_{A_1,\ldots,A_k}$ be the polygonal line whose vertices are $A_1, \ldots, A_k$. Then the computed elongations $\mathcal{E}(P_{A_1,\ldots,A_{k-1},A_k})$ converge if $\max\{|A_iA_{i+1}|, 1 \le i < k\} \to 0$ is provided. More precisely,

$$\lim_{\max\{|A_iA_{i+1}|, 1\le i<k\}\to 0} \mathcal{E}(P_{A_1,\ldots,A_k})$$
$$= \frac{\mathcal{L}ength(\rho) + \sqrt{\left(\oint_\rho \frac{2\dot{x}\dot{y}}{\dot{x}^2+\dot{y}^2}ds\right)^2 + \left(\oint_\rho \frac{\dot{x}^2-\dot{y}^2}{\dot{x}^2+\dot{y}^2}ds\right)^2}}{\mathcal{L}ength(\rho) - \sqrt{\left(\oint_\rho \frac{2\dot{x}\dot{y}}{\dot{x}^2+\dot{y}^2}ds\right)^2 + \left(\oint_\rho \frac{\dot{x}^2-\dot{y}^2}{\dot{x}^2+\dot{y}^2}ds\right)^2}}$$
$$= \frac{\mathcal{L}ength(\rho) + \sqrt{\left(\int_a^b \frac{2\dot{x}\dot{y}}{\dot{x}^2+\dot{y}^2}dt\right)^2 + \left(\int_a^b \frac{\dot{x}^2-\dot{y}^2}{\dot{x}^2+\dot{y}^2}dt\right)^2}}{\mathcal{L}ength(\rho) - \sqrt{\left(\int_a^b \frac{2\dot{x}\dot{y}}{\dot{x}^2+\dot{y}^2}dt\right)^2 + \left(\int_a^b \frac{\dot{x}^2-\dot{y}^2}{\dot{x}^2+\dot{y}^2}dt\right)^2}} \qquad (15)$$

where $\mathcal{L}ength(\rho)$ is the length of the curve ρ.

Proof For each polygonal curve $P_{A_1,\ldots,P_k}$ we have

$$\lim_{\max\{|A_iA_{i+1}|, 1\le i<k\}\to 0} \sum_{i=1}^{k-1} |A_iA_{i+1}| = \mathcal{L}ength(P_{A_1,\ldots,A_k}) \qquad (16)$$

where $\mathcal{L}ength(P_{A_1,\ldots,A_k})$ denotes the length of the polygonal line $P_{A_1,\ldots,A_k}$.

Furthermore, by using the trigonometric identities (13) and well-known fact that the first derivative $\frac{\dot{y}}{\dot{x}}$ of a curve $x = x(t)$, $y = y(t)$ equals the tangent of the angle between the curve tangent and the x-axis, and by applying (14) we have

$$\lim_{\substack{k\to\infty \\ \max\{|A_iA_{i+1}|, 1\le i<k\}\to 0}} \sum_{i=1}^{k-1} |A_iA_{i+1}| \cdot \sin(2\alpha_i)$$
$$= \oint_C \frac{2\dot{x}\dot{y}}{\dot{x}^2+\dot{y}^2}ds = \int_a^b \frac{2\dot{x}\dot{y}}{\sqrt{\dot{x}^2+\dot{y}^2}}dt, \qquad (17)$$

$$\lim_{\substack{k\to\infty \\ \max\{|A_iA_{i+1}|, 1\le i<k\}\to 0}} \sum_{i=1}^{k-1} |A_iA_{i+1}| \cdot \cos(2\alpha_i)$$
$$= \oint_C \frac{\dot{x}^2-\dot{y}^2}{\dot{x}^2+\dot{y}^2}ds = \int_a^b \frac{\dot{x}^2-\dot{y}^2}{\sqrt{\dot{x}^2+\dot{y}^2}}dt. \qquad (18)$$

Entering (16)–(18) into (10) we establish the proof. □

We will illustrate the statement of Theorem 5.1 by the following example—see Fig. 4.

Example Fifty points x_i are selected at random three times. The polygonal line having vertices $(0, 0) = (x_1, x_1^2)$, $(x_2, x_2^2), \ldots, (x_{49}, x_{49}^2)$, $(x_{50}, x_{50}^2) = (1, 1)$ is oriented by the new method. The following elongations are computed:

Fig. 7(a) The computed elongation is **11.26**. The abscissas of the selected points are:

0, 0.01548, 0.03768, 0.1714, 0.17163, 0.25785, 0.27185, 0.2785, 0.28133, 0.30199, 0.30501, 0.36028, 0.3729, 0.4025, 0.42834, .440952, 0.44444, 0.44854, 0.4561, 0.46496, 0.52758, 0.54522, 0.5477, 0.57911, 0.59521, 0.60459, 0.6282, 0.65274, 0.68177, 0.68867, 0.70455, 0.70498, 0.7217, 0.72928, 0.78194, 0.80431, 0.8188, 0.81885, 0.82833, 0.84286, 0.86448, 0.87797, 0.8859, 0.89792, 0.90586, 0.91493, 0.9265, 0.93262, 0.96803, 1.

Fig. 7(b) The computed elongation is **11.21**. The abscissas of the selected points are:

0, 0.01958, 0.03698, 0.04119, 0.09771, 0.14122, 0.16451, 0.19403, 0.22791, 0.25548, 0.26089, 0.27497, 0.3218, 0.3474, 0.35739, 0.36247, 0.41977, 0.43108, 0.43763,

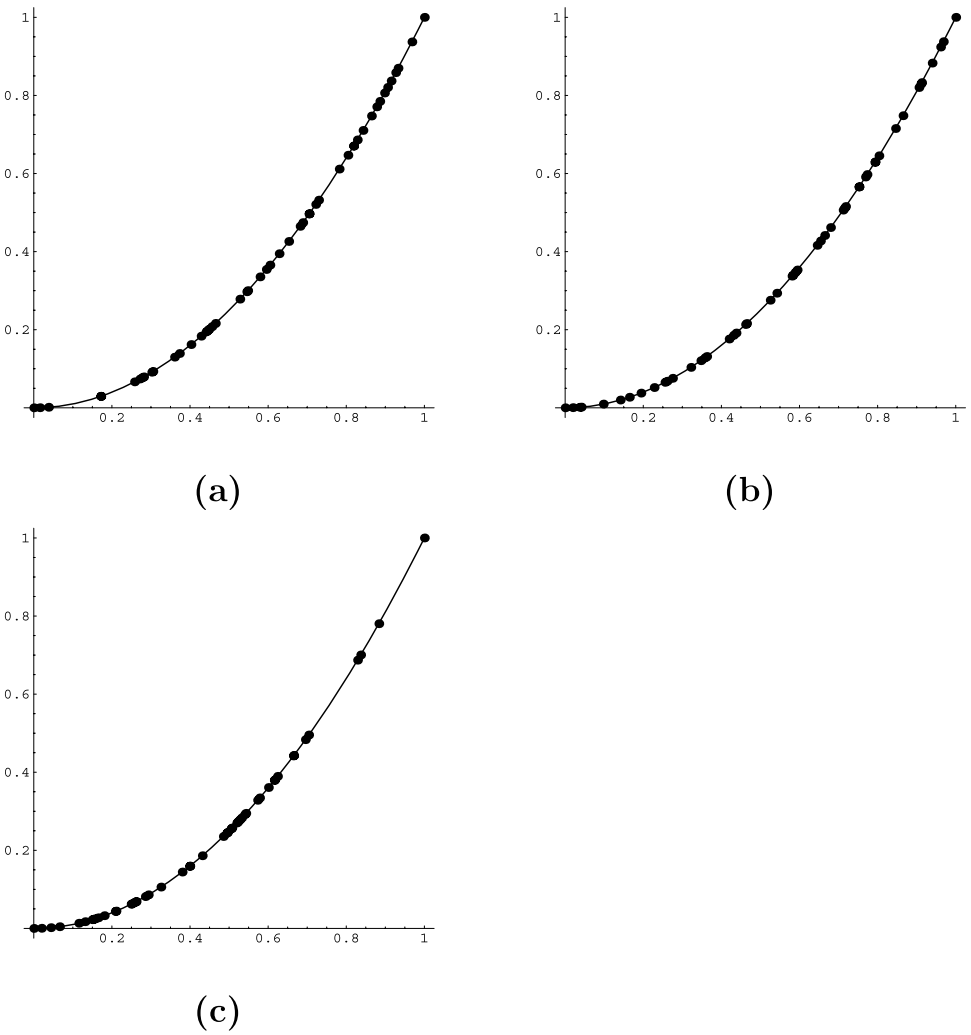

Fig. 4 Fifty randomly selected points (x_i, x_i^2) are displayed. The polygonal line $(0,0) = (x_1, x_1^2), (x_2, x_2^2), \ldots, (x_{49}, x_{49}^2), (x_{50}, x_{50}^2) = (1,1)$ is measured by the new method. The following convergent measured elongations are obtained: **a** 11.26, **b** 11.22, and **c** 11.22. If the elongation is measured by using $F_{0,2}(\alpha, P)$ then the following divergent elongations are measured: **a** 8.29, **b** 13.57, **c** 26.54

0.46182, 0.46467, 0.52494, 0.54177, 0.58073, 0.58357, 0.58912, 0.59408, 0.64511, 0.6537, 0.66437, 0.67948, 0.71158, 0.71524, 0.71797, 0.75207, 0.75233, 0.76885, 0.77291, 0.79283, 0.79366, 0.80336, 0.84576, 0.86491, 0.90572, 0.91077, 0.9126, 0.9396, 0.96122, 0.96832, 1.

Fig. 7(c) The computed elongation is **11.22**. The abscissas of the selected points are:

0, 0.01977, 0.04359, 0.06601, 0.11522, 0.13125, 0.14959, 0.15277, 0.15703, 0.16493, 0.18058, 0.20863, 0.21061, 0.24919, 0.25102, 0.25721, 0.26061, 0.26216, 0.28553, 0.29327, 0.32544, 0.37996, 0.39886, 0.39959, 0.43143, 0.4852, 0.49406, 0.49615, 0.50489, 0.50712, 0.5197, 0.52295, 0.52722, 0.53215, 0.53999, 0.54289, 0.57292, 0.57815, 0.60073, 0.670, 0.61667, 0.62405, 0.66466, 0.66548, 0.69530, 0.70383, 0.82888, 0.8369, 0.88341, 1.

As expected, because of the satisfied convergence property all three obtained values (11.26, 11.21, and 11.22) are similar and very close to the numerically obtained 11.2266 value.

Let us mention that the convergence property would not be satisfied if the elongation is derived by using $F_{2,0}(\alpha, P)$ and defined as

$$\mathcal{E}_{2,0}(P) = \frac{\max\{F_{0,2}(\alpha, P) \mid \varphi \in [0, 2\cdot\pi]\}}{\min\{F_{0,2}(\alpha, P) \mid \varphi \in [0, 2\cdot\pi]\}}. \tag{19}$$

For the polygonal lines whose vertices are presented in Fig. 4 the following elongations are computed: (a) (8.29), (b) (13.57), (c) (26.54), illustrating that the elongation measure $\mathcal{E}_{2,0}$ defined by (19) does not have the convergence property.

The previous theorem is said to be the main result of the paper because it enables a closed formula for computing elongation. This formula can also be applied to open curves and curves consisting of several curve segment. If restricted to polygonal curves, the new definition is consistent with Definition 3.1 and it can be computed by using (10). Thus, we give the next definition.

Definition 5.1 Assume that we have a piecevise smooth enough curve ρ given in a parametric form $x = x(t)$, $y =$

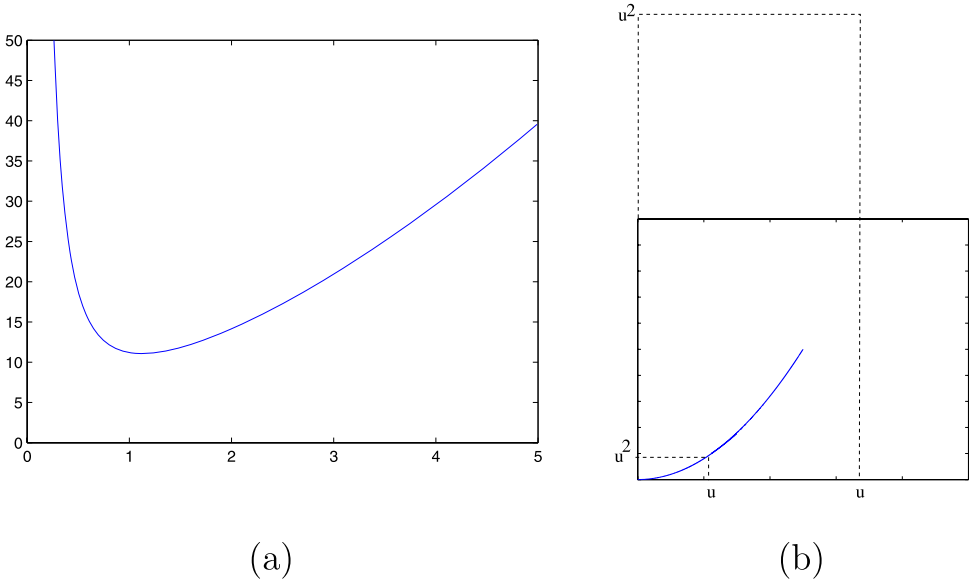

Fig. 5 **a** The graph of $\mathcal{E}(P(u))$ is presented. **b** illustrates that in both cases, when u is either very big or very small, the graph of $P(u)$ belongs to a very elongated rectangle which indicates that the measured elongation should be very high

$y(t)$, $(t \in [a,b])$. The elongation $\mathcal{E}(\rho)$ of the curve ρ is defined as

$$\mathcal{E}(\rho) = \frac{\mathcal{L}ength(\rho) + \sqrt{\left(\oint_\rho \frac{2\dot{x}\dot{y}}{\dot{x}^2+\dot{y}^2}ds\right)^2 + \left(\oint_\rho \frac{\dot{x}^2-\dot{y}^2}{\dot{x}^2+\dot{y}^2}ds\right)^2}}{\mathcal{L}ength(\rho) - \sqrt{\left(\oint_\rho \frac{2\dot{x}\dot{y}}{\dot{x}^2+\dot{y}^2}ds\right)^2 + \left(\oint_\rho \frac{\dot{x}^2-\dot{y}^2}{\dot{x}^2+\dot{y}^2}ds\right)^2}}$$

$$= \frac{\mathcal{L}ength(\rho) + \sqrt{\left(\int_a^b \frac{2\dot{x}\dot{y}}{\sqrt{\dot{x}^2+\dot{y}^2}}dt\right)^2 + \left(\int_a^b \frac{\dot{x}^2-\dot{y}^2}{\sqrt{\dot{x}^2+\dot{y}^2}}dt\right)^2}}{\mathcal{L}ength(\rho) - \sqrt{\left(\int_a^b \frac{2\dot{x}\dot{y}}{\sqrt{\dot{x}^2+\dot{y}^2}}dt\right)^2 + \left(\int_a^b \frac{\dot{x}^2-\dot{y}^2}{\sqrt{\dot{x}^2+\dot{y}^2}}dt\right)^2}}.$$

Remark 5.1 New definition for measuring of elongation of an arbitrary curve, as given by Definition 5.1, involves first derivatives $\dot{x}(t)$ and $\dot{y}(t)$ for curves given in a parametric form $x = x(t)$, $y = y(t)$. This is not a problem when working with curves described formally by the equations, as it happens in computer graphics where equations of the curves used are known very often. On the other side, the computing (estimating) first derivatives when working with sample (discrete) data is usually a big problem. This remark should point out that an efficient estimation of $\mathcal{E}(\rho)$ does not need computation (estimation) of the appearing derivatives. As it has been stated by Theorem 5.1, the elongation measure $\mathcal{E}(\rho)$ can be estimated efficiently by a computation of $\mathcal{E}(P_{A_1,\ldots,A_k})$ if the set of sample points $A_1,\ldots,A_k$ is dense enough on the curve ρ. The computation of $\mathcal{E}(P_{A_1,\ldots,A_k})$ by using the equation (10) is simple, fast, does not involve the first derivative approximations, and guaranties the convergence $\mathcal{E}(P_{A_1,\ldots,A_k}) \to \mathcal{E}(\rho)$.

As an illustration of the behavior of shape elongation given by Definition 5.1 we give the following synthetic example. Let us consider a parabola segment $P(u)$ $y = x^2$ on the interval $[0,u)$, where u varies from 0 to infinity. The graph of $\mathcal{E}(P(u))$ is presented in Fig. 5(a). As it can be seen, for a very small u close to 0, the measured elongation is very high and tends to infinity as u tends to 0. After that, $\mathcal{E}(P(u))$ decrease and reaches the minimum somewhere close to 1. After that $\mathcal{E}(P(u))$ increases again, and tends to infinity if u tends to infinity, too.

Such a behavior is expected. Indeed, for a very small u, the parabola segment $P(u)$ is contained in a very elongated rectangle whose sides are u and u^2. If u becomes very big, then the rectangle that includes $P(u)$ is again very elongated because the ratio of its sides u^2 and u is again very big (see Fig. 5(b)).

At the end of this section will consider some problems that could appear when compute $\mathcal{E}(P)$.

First we start with the noise problems. Generally speaking, all methods that use only boundary information must be sensitive to boundary changes (e.g. deformations, intrusions, noise, etc.). Inevitably, once we accept to work with boundary informations and exploit the benefits that come from sensitive methods, we have also to accept problems which could come from the boundary sensitivity. Typical problems are caused by a noise on images that should be processed. Some of problems when dealing with a noise shape can be avoid by a suitable choice of polygonal approximation or by applying some standard procedures (e.g. smoothing). Some noise effects to the computed shape elongation are illustrated on Fig. 6. It can be seen that a small noise could be acceptable for a still efficient elongation estimation (Fig. 6(b)) while a high noise could lead to an essential error (Fig. 6(d)).

Another disadvantage of the method presented here could be the fact that the new elongation measure depends on the edge lengths and the edge orientations but not on the order of edges. Thus, the following lemma holds.

Fig. 6 Computed elongations $\mathcal{E}(P)$ are given to illustrate noise effects

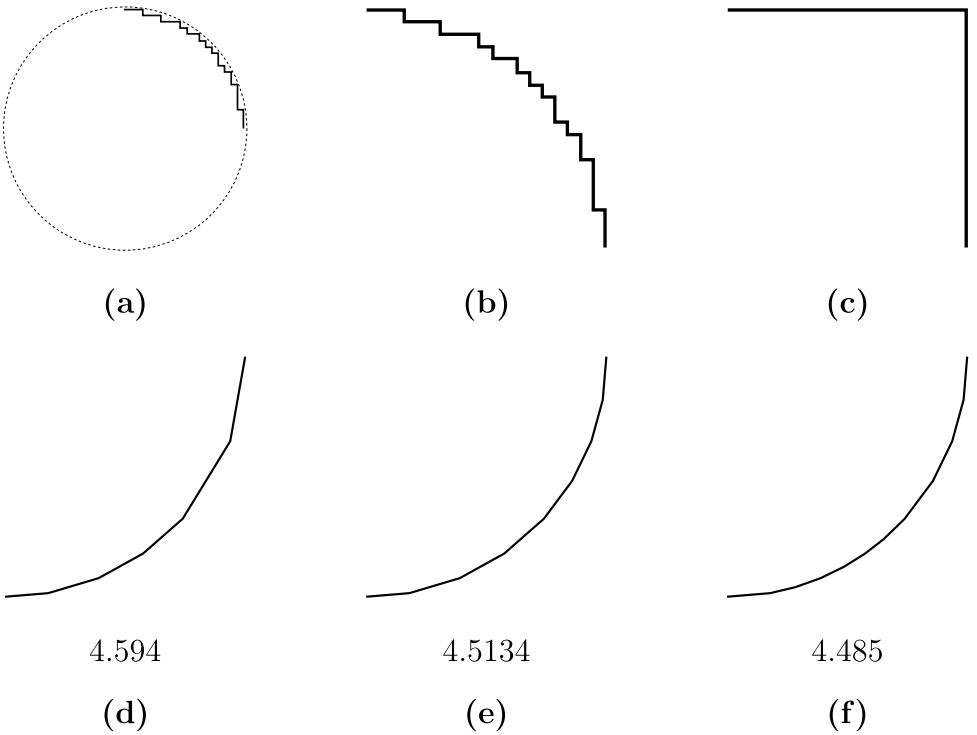

Fig. 7 Computed elongations $\mathcal{E}$ for shapes (**b**) and (**c**) that consist of 19 vertical and 19 horizontal unit edges are both equal 1. The digitized circular arc in (**b**) is approximated by the Ramer algorithm (arcs (**d**), (**e**), (**f**)) and computed values are closer to the exact elongation value ($\frac{\pi+2}{\pi-2} \approx 4.5039$) of an ideal arc as the threshold level in the Ramer algorithm decrease

Lemma 5.1 *Let P be a polygonal boundary. Then the measured elongation $\mathcal{E}(P)$ has the same value for all permutations of edges of P.*

Notice that if P is closed polygon then all permutations of edges of P do not necessarily give a closed polygon again (the result can be an open polygonal line or a self-intersecting polygonal line), but the elongation of such resulting polygonal lines still can be measured by $\mathcal{E}$. Also, it is worth mentioning that a request that a given shape descriptor assigns different values for (essentially) different shapes is very reasonable but, in practice, is difficult to be achieved. More precisely, up to our knowledge, there is no created descriptor which reaches our perception in all situations.

A generalization of Lemma 5.1 is the following lemma.

Lemma 5.2 *Let a polygon $P = (e_1, \ldots, e_n)$ be a polygonal boundary, e_i an arbitrary, fixed edge of P and $f_1, \ldots, f_k$ be a set of edges with same slope as the slope of e_i and the total sum of edge lengths equal to $|e_i|$ (i.e. $\sum_{1\le j\le k} |f_j| = |e_i|$). Then the elongation $\mathcal{E}(P)$ equals the elongation of all the polygonal lines consisting of edges $\{e_l \mid 1 \le l \le n, l \ne i\} \cup \{f_j \mid 1 \le j \le k\}$.*

The situation described by Lemma 5.2 is illustrated by Fig. 7. A digitalization (see [9]) of the south-east arc of a circle is presented in Fig. 7(b). It consists of 19 vertical and 19 horizontal unit edges. If those edges are listed in the order: 19 horizontal edges first, after that 19 vertical edges, we get the polygonal line presented in Fig. 7(c). Due to Lemma 5.2, both polygonal lines have the same measured elongation equal to 1, which is not preferred.

Such an unprefered elongation of shape in Fig. 7(b) can be corrected if a suitable polygonal approximation of the presented digital arc is applied. In Fig. 7(d)–(f) the Ramer [12] algorithm is applied for three different threshold values: 2, 4, and 8. The following computed elongations are obtained: 4.4595, 4.5134, and 4.485, respectively. It can be

seen that a decrease of the threshold value in the Ramer algorithm lead to the measured elongations which are closer to the theoretical value $\frac{\pi+2}{\pi-2} \approx 4.5039$ for the measured elongation of the south-east arc of a circle. This (exact) theoretical value $\frac{\pi+2}{\pi-2}$ is obtained by applying the formula from Definition 5.1. Notice that any reasonably good polygonal approximation algorithm will keep the shape in Fig. 6(c) almost unchanged and, consequently, the corresponded measured elongations would always be close to 1.

Problems similar to the previously discussed one would happen if we work with digital curves that are presented by the Freeman eight chain code [4, 9] where the shape boundary is represented by edges having the lengths 1 (if their slopes are $k \cdot 90°$, $k = 0, 1, 2, 3$) or $\sqrt{2}$ (if their slopes are $k \cdot 45°$, $k = 1, 3, 5, 7$). The computed elongation $\mathcal{E}$ would depend only on the numbers $n_0, \ldots, n_7$ of the edges from a particular class (determined by the belonging edge slopes). Similarly as above, those problems can be avoid by a use of a proper polygonal approximation.

To close this section, let us mention that such a phenomena on curve measures are expected and easy to construct. Very often, so called, 'zig-zag' curves are used for an illustration and construction. Indeed, even if we use a digitalization presented in Fig. 7(b) for estimating a very basic descriptor, as the length of the digitized arc (see [3]) is, we would obtain 38, what is far away from the exact length $\frac{38\pi}{4} \approx 29.8451$ of the arc. Of course, the better estimates would be obtained by a suitable polygonal approximation.

6 Conclusion

In this paper we have been dealing with shape elongation which is one of the basic shape descriptors. The traditional shape elongation measure is area based, and therefore defined only for closed shapes. Here we introduced a boundary based elongation measure for arbitrary shapes. Using our method, elongation can be measured for shapes having partially extracted boundaries, but also for shapes composed of several components. The measure is invariant with respect to rotation, translation and scaling. Also, the closed formula for computation exists and it expresses the shape elongation as

$$\frac{\mathcal{L}ength(\rho) + \sqrt{\left(\int_a^b \frac{2\dot{x}\dot{y}}{\sqrt{\dot{x}^2+\dot{y}^2}}dt\right)^2 + \left(\int_a^b \frac{\dot{x}^2-\dot{y}^2}{\sqrt{\dot{x}^2+\dot{y}^2}}dt\right)^2}}{\mathcal{L}ength(\rho) - \sqrt{\left(\int_a^b \frac{2\dot{x}\dot{y}}{\sqrt{\dot{x}^2+\dot{y}^2}}dt\right)^2 + \left(\int_a^b \frac{\dot{x}^2-\dot{y}^2}{\sqrt{\dot{x}^2+\dot{y}^2}}dt\right)^2}}.$$

The above formula can be understood as even simpler than the formula for the standard method (expression (3) for centralized moments should be entered into (4)).

To close, we would like to point out that the new measure is not developed in order to be dominant to the standard one. It is clear that when working with shape descriptors, it is not always possible to have a perfect or best measure. All shape descriptors have their strengths and their weakness while their usefulness is in a strong relation to the suitability of particular applications.

Furthermore, the new measure is not developed ultimately to be an alternative to the standard measure. It is not difficult to imagine a situation where both measures could be used to form useful conclusions from their mutual relation.

Acknowledgements The authors thank to the referees for their valuable suggestions that lead to improvements of the paper. Also, the authors are thankful to Dr Paul L. Rosin for providing some of experimental results.

References

1. Bandt, S., Laaksonen, J., Oja, E.: Statistical shape features for content-based image retrieval. J. Math. Imaging Vis. **17**, 187–198 (2002)
2. Boxer, L.: Computing deviations from convexity in polygons. Pattern Recognit. Lett. **14**, 163–167 (1993)
3. Coeurjolly, D., Klette, R.: A comparative evaluation of length estimators of digital curves. IEEE Trans. Pattern Anal. Mach. Intell. **26**(2), 252–257 (2004)
4. Freeman, H.: Boundary encoding and processing. In: Lipkin, B.S., Rosenfeld, A. (eds.) Picture Processing and Psyhopictorics, pp. 391–402. Academic Press, New York (1970)
5. Freeman, H., Shapira, R.: Determining the minimum-area encasing rectangle for an arbitrary closed curve. Commun. ACM **18**, 409–413 (1975)
6. Horn, B.K.P.: Robot Vision. MIT Press, Cambridge (1986)
7. Jain, R., Kasturi, R., Schunck, B.G.: Machine Vision. McGraw-Hill, New York (1995)
8. Kakarala, R.: Testing for convexity with Fourier descriptors. Electron. Lett. **14**, 1392–1393 (1998)
9. Klette, R., Rosenfeld, A.: Digital Geometry. Kaufmann, San Francisco (2004)
10. Martin, R.R., Stephenson, P.C.: Putting objects into boxes. Comput. Aided Des. **20**, 506–514 (1988)
11. Rahtu, E., Salo, M., Heikkilä, J.: A new convexity measure based on a probabilistic interpretation of images. IEEE Trans. Pattern Anal. Mach. Intell. **28**, 1501–1512 (2006)
12. Ramer, U.: An iterative procedure for the polygonal approximation of plane curves. Comput. Graph. Image Process. **1**, 244–256 (1972)
13. Rosin, P.L.: Techniques for assessing polygonal approximations of curves. IEEE Trans. Pattern Anal. Mach. Intell. **19**(6), 659–666 (1997)
14. Rosin, P.L.: Measuring shape: ellipticity, rectangularity, and triangularity. Mach. Vis. Appl. **14**, 172–184 (2003)
15. Rosin, P.L., Mumford, C.L.: A symmetric convexity measure. Comput. Vis. Image Underst. **103**, 101–111 (2006)
16. Stojmenović, M., Žunić, J.: New measure for shape elongation. In: IbPRIA 2007, 3rd Iberian Conference on Pattern Recognition and Image Analysis. Lecture Notes in Computer Science, vol. 4478, pp. 572–579 (2007)
17. Sonka, M., Hlavac, V., Boyle, R.: Image Processing, Analysis, and Machine Vision. Chapman and Hall, London (1993)
18. Tsai, W.H., Chou, S.L.: Detection of generalized principal axes in rotationally symmetric shapes. Pattern Recognit. **24**, 95–104 (1991)

19. Žunić, J., Kopanja, L., Fieldsend, J.E.: Notes on shape orientation where the standard method does not work. Pattern Recognit. **39**(5), 856–865 (2006)
20. Žunić, J.: Boundary based orientation of polygonal shapes. In: Lecture Notes in Computer Science, Hsinchu, Taiwan, PSIVT, December 2006, pp. 108–117 (2006)
21. Žunić, J., Rosin, P.L.: A new convexity measurement for polygons. IEEE Trans. Pattern Anal. Mach. Intell. **26**, 923–934 (2004)
22. Žunić, J., Stojmenović, M.: Boundary based shape orientation. Pattern Recognit. (2007). doi:10.1016/j.patcog.2007.10.007

Miloš Stojmenović received the Bachelor of Computer Science degree at the School of Information Technology and Engineering, University of Ottawa, in 2003. He obtained his Master's degree in computer science at Carleton University in Ottawa, Canada in 2005, and is now completing his PhD in the same field at the University of Ottawa. He has a long list of awards for academic performance and medals from chess and math competitions. He published over a dozen articles in the fields of computer vision, image processing, and wireless networks. More details can be found at www.site.uottawa.ca/ mstoj075.

Joviša Žunić received the MSc and PhD degrees in mathematics and computer science from the University of Novi Sad (Serbia) in 1989 and 1991, respectively. He worked as a professor and researcher at the University of Novi Sad for more than a decade and is currently a senior lecturer in Department of Computer Science at Exeter University. He is also with the Mathematical Institute of the Serbian Academy of Sciences and Arts.

His research interest are in computer vision and image processing, digital geometry, shape representation and encoding of digital objects, discrete mathematics, combinatorial optimization, wireless networks, neural networks, and number theory.